An influence of the different incoming wake-like flows on the rotor vibrations

Paper

Naumov, I. V.; Kabardin, Ivan K. ; Mikkelsen, Robert Flemming; Okulov, Valery; Sørensen, Jens Nørkær

Published in:
Wake Conference 2017

Link to article, DOI:
10.1088/1742-6596/854/1/012034

Publication date:
2017

Document Version
Publisher's PDF, also known as Version of record

An influence of the different incoming wake-like flows on the rotor vibrations

2017 J. Phys.: Conf. Ser. 854 012034

(http://iopscience.iop.org/1742-6596/854/1/012034)

An influence of the different incoming wake-like flows on the rotor vibrations

I V Naumov[1], I K Kabardin[1], R F Mikkelsen[2], V L Okulov[1,2], J N Sørensen[2]

[1]Kutateladze Institute of Thermophysics, SB RAS, Novosibirsk 630090, Russia
[2]Department of Wind Energy, Technical University of Denmark, 2800 Lyngby, Denmark

E-mail: naumov@itp.nsc.ru

Abstract. The aim of the current investigation is the rotor vibrations generated by the disturbances caused the different types of incoming wake-like flows. Those wakes arriving at the tested rotor were created by two ways: a passive wake generator (immobile disk) and an upstream rotating rotor as an active wake generator. The influence of both wakes on the tested rotor was studied in a water flume. A model of the tested three-bladed rotor designed using Glauert's optimum theory at an optimal tip speed ratio $\lambda = 5$ was placed in both "passive" and "active" wakes to recognize dissimilarities on the vibrations of the tested rotor. The distance from the wake generators to the tested rotor was varied from 4 to 8 rotor diameters. Also, the shift between the rotor axis and axis of the incoming wakes was changed to 0, 0.5 and 1 rotor diameters. The flow condition before rotor was measured with high temporal accuracy using LDA. The turbulent intensity of the incoming wake flows changed from 3 to 16% due to the types of the wake generators. Power and thrust characteristics and their pulsations of the tested rotor were measured by strain gauges. The dependences of power coefficients from tip speed ratios and positions of the wake generators were documented. The present study showed a strong influence of the initial flow from the two different wake generators on the rotor vibrations.

1. Introduction

Wind turbines are often sited near obstacles such as forests, ridges, hills and cliffs [1]. Some of them can be very favorable for producing the wind power but other ones must be strictly avoided since they can generate considerable stagnation of flow ("wind shade") in the rotor area (fig. 1). Next factor is that the obstacles appearing before the wind turbine rotor cause turbulence level increasing. The turbine efficiency depends on the nature of the turbulence. An effect of increasing the level of free-stream turbulence may lead to an earlier breaking vortex wake behind a wind turbine, which is very important for the arrangement of wind parks [2, 3].

With regard to the wind-farm developments, there is an increasing interest in studying the interaction and the power degeneration between two or more interacting wind turbines [4, 5]. The background is that the power degradation caused by the influence of the wakes has become a major subject in the design process of wind farms. Wind turbines are usually located in a wind farm to save space, to simplify the energy transfer and also to reduce the costs of an installation and maintenance of the wind turbines. The distance between the nearest wind turbines typically ranges from 3 to 10 rotor

diameters. The adverse effect appears when the inner wind turbines situated downstream of the forward ones and interact with strong rotor wakes. Numerous studies have reported a significant effect of external pulsations on power characteristics of wind turbines [6].

The present paper continues our previous experimental studies in the water flume of the flow structures around the different dual disk-rotor or rotor-rotor configurations to establish this new aspect of the rotor operations. The setup and experiment conditions are in detail described in [7-10] where only the flow properties and average torque and thrust of the tested rotor have been experienced. A model of the three-bladed rotor designed using Glauert's optimum theory at a tip speed ratio $\lambda = 5$ was placed in the different wakes behind the passive solid disk and the rotating upstream rotor as the active wake generator.

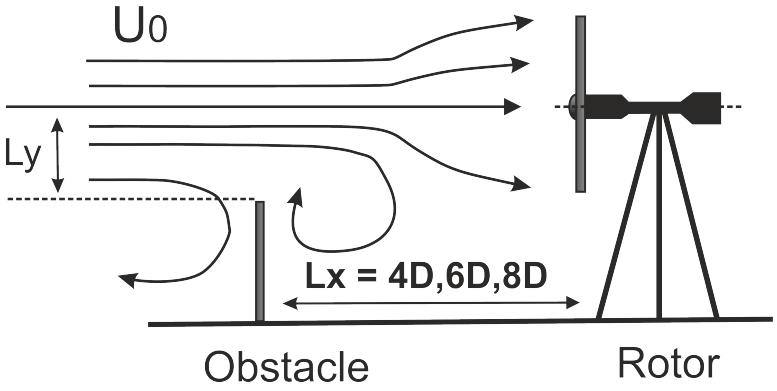

Figure 1. The schematic of the problem.

The purpose of the present investigation is to determine the rotor performance due to the interaction with the two types of the wakes. In our experiments, both active and passive wake generators (rotating rotor or immobile disk with the diameter close to the tested rotor) were used as the different oscillators in the upstream flow to recognize a dissimilarity in vibrations of the tested rotor. The wake influence has also been studied at the different distances between the tested rotor and wake generators or shifts of the rotor and wake axis. At first, by laser Doppler anemometry (LDA) method, we examined a structure and oscillations of the flow disturbances coming from both wake generators. The turbulent intensity of the incoming flow changed from 3 to 16 %. Then torque and thrust and their pulsation were measured by strain gauges. The dependences of power coefficients from tip speed ratio and the positions of the wake generators were studied. The present study also showed a strong influence of the types of the wake generators on the rotor vibrations. This conclusion is based on our comparison of the vibration of the tested rotor initiated by the Strouhal flow oscillations inherited to both disk or rotor wakes [11] and a blade frequency generated only in the rotor wakes. The detailed experimental description and main results are presented below.

2. Experimental Method and Results

The experiments were carried out in a water flume (fig. 2a, b). The length of the flume is 35 m, width is 3 m, and height is 1.0 m with 3 m transparent walls in the test section. A detailed characterization of the water flume flow can be found in [7-10]. The initial flow in the flume was subject to alow turbulence level within 2.5%, limiting the influence of external disturbances on the development of the inherent wake instability. The tested rotor was positioned downstream the wake generators. The three-bladed tested rotor has a diameter $D = 2R = 0.376$m, the blades consisting of SD7003 airfoil sections were specially designed for optimum operating conditions at the tip speed ratio $\lambda = 5$ [9, 10], where $\lambda = \Omega R/U_0$, and Ω is the angular speed of the rotor. The Reynolds numbers based on rotor diameter and the initial flow in the flume vary in the range $140.000 < Re < 240.000$.

The same rotor or disk with a diameter close to the rotor (0.9D) was used as the active and passive wake generators. The properties of the wake behind of the single rotor or disk are well known and they were studied in our previous work [7-10]. The setup location (fig. 2.a) at a height of 0.5 m from the flume bottom and at a distance of 1.5 m from the flume wall allows avoiding an influence of the boundary layer, whose thickness did not exceed 0.2 m from the bottom and the walls of the flume [9, 10]. The boundary layer influences on the entire flow pattern and changes the influence of the upstream obstacle on the investigated rotor; therefore, in some respect we here chose to research without the boundary layer influence. A ratio of the rotor area (0.111 m^2) and the area of the flume cross-section (3 m^2) is only 3.7%. For this reason, a blockage effect and other influences of the flume walls are actually very small and no corrections are made.

The wake generator and tested rotor are mounted on a platform displaced along the flume for different fixed distances between obstacle and rotor (fig. 2.a, b). The wake generator (disk or rotor 1) was axially placed at different positions Lx=4D, 6D and 8D infront of the wake affected rotor (fig. 2a). In other tests, the generator was placed at one fixed distance of 6 diameters upstream the rotor, withthe generator axis shifted from the rotor axis by Ly=0.5D and 1D (fig. 2b). The influence of the wake on the rotor performance and the thrust characteristics has been studied at the different positions (Lx and Ly) of the wake generator and tested rotor.

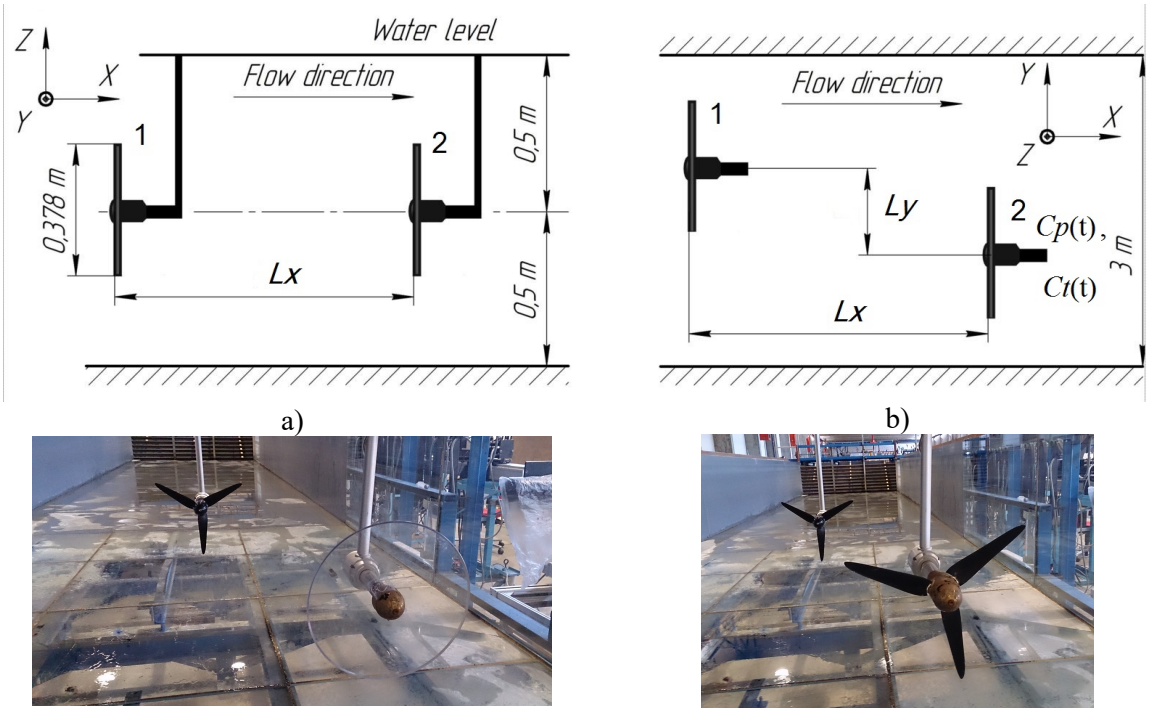

Figure 2. The schematic and photos of the experimental setup 1- obstacle disk or rotor, 2- three-bladed rotor.

At first, the velocity of the flow incoming to the tasting rotor was measured with high temporal accuracy using LDA. The initial free flow in the setup area of the flume has a uniform profile with velocity U_0 = 0.54 m/s and turbulence level 3 % [10]. The LDA measurements were carried out to find a deformation of the velocity profile by both wake generators. The local history of the axial velocity in each point was obtained using a Dantec 2-D Fiber flow LDA, based on a 1W Argon laser with a differential optical configuration and a frequency shift of 40 MHz. The diameter of the optical gauge is 112 mm and the focal length is 600 mm with a beam diameter of 1.35 mm. The wavelength of the laser beam is 514.5 nm (green light). The size of the probing optical field was 0.12×0.12×1.52 mm^3. These LDA measurements of both velocity and oscillations (RMS) are shown in fig.3 and fig.4.

The velocity profiles were measured at a distance of 0.5 D upstream of the tested rotor. The velocity is reduced up to 55 % with velocity oscillations growing up to 24% when the wake generator is an immobile disk and the tested rotor placed on the same axis (Ly = 0). The velocity was found to reduce up to 80 % when the rotating rotor was used as the active wake generator placed on the same axis. The level of RMS for the wake varied in the range from 3 to 16 % and becomes close to the turbulence intensity of the free flow when Lx=8D for both types of wake generators (fig. 3c). LDA velocity profiles of the rotor wake for different tip speed ratio at Lx = 6D (fig. 3d) show that the value of tip speed ratio almost does not influence the velocity attenuation in the wake.

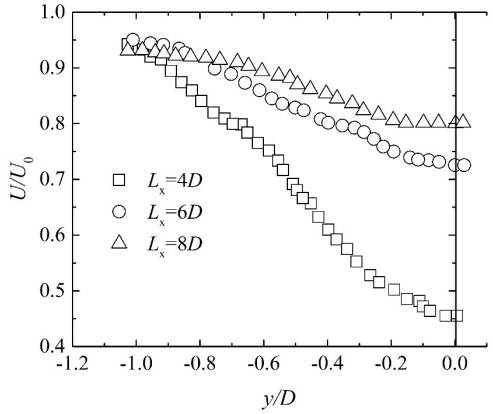

Figure 3a. LDA velocity profiles behind the passive wake generator – immobile disk.

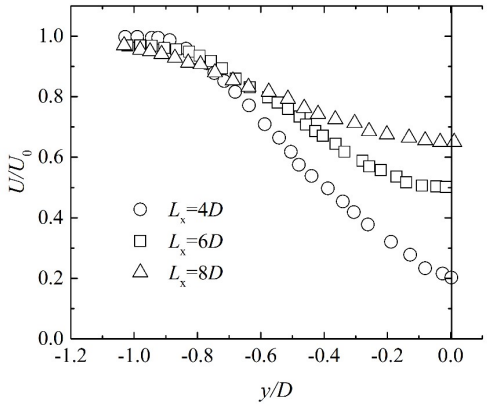

Figure 3b. LDA velocity profiles behind the active wake generator – rotating rotor.

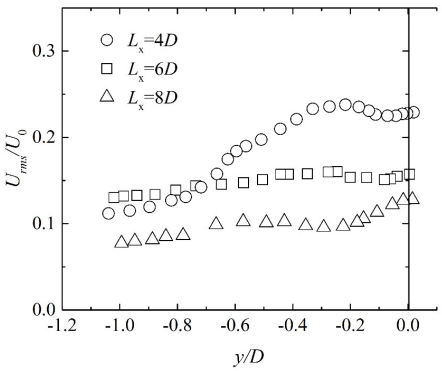

Figure 3c. RMS of LDA velocity behind the passive wake generator - immobile disk.

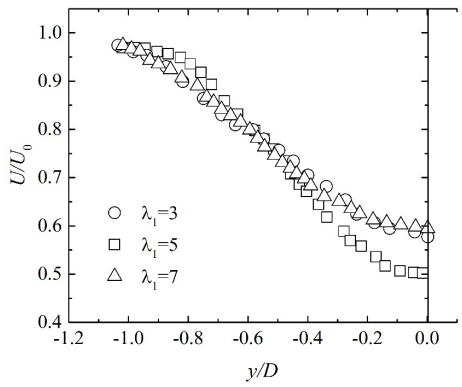

Figure 3d. LDA velocity profiles behind the rotating rotor for different tip speed ratio at Lx=6D.

Measured LDA velocity profiles with the axis of both passive and active wake generators shifted from the axis of the tested rotor at the different distances, are shown in fig. 4. From these dependencies, it can be seen that at Lx=4D both types of wake generators have a strong influence on the flow velocity profile and the active rotor extract more energy from the flow. It can be explained by the tip vortex system produced by the active rotor which does not inherit to the passive wake behind the disk. The velocity decrease in the wake is up to 40 % for the passive disk case and up to 20 % for the active rotor. The velocity attenuation in the rotor axis decreases only to 87 % for the disk and to 80 % for the rotor when Ly=0.5D. At Ly = 1D the velocity attenuation almost disappears in the rotor area for both passive and active types of wake generators (fig. 3a-c). For Lx=6D the velocity attenuation decreases up to two times.

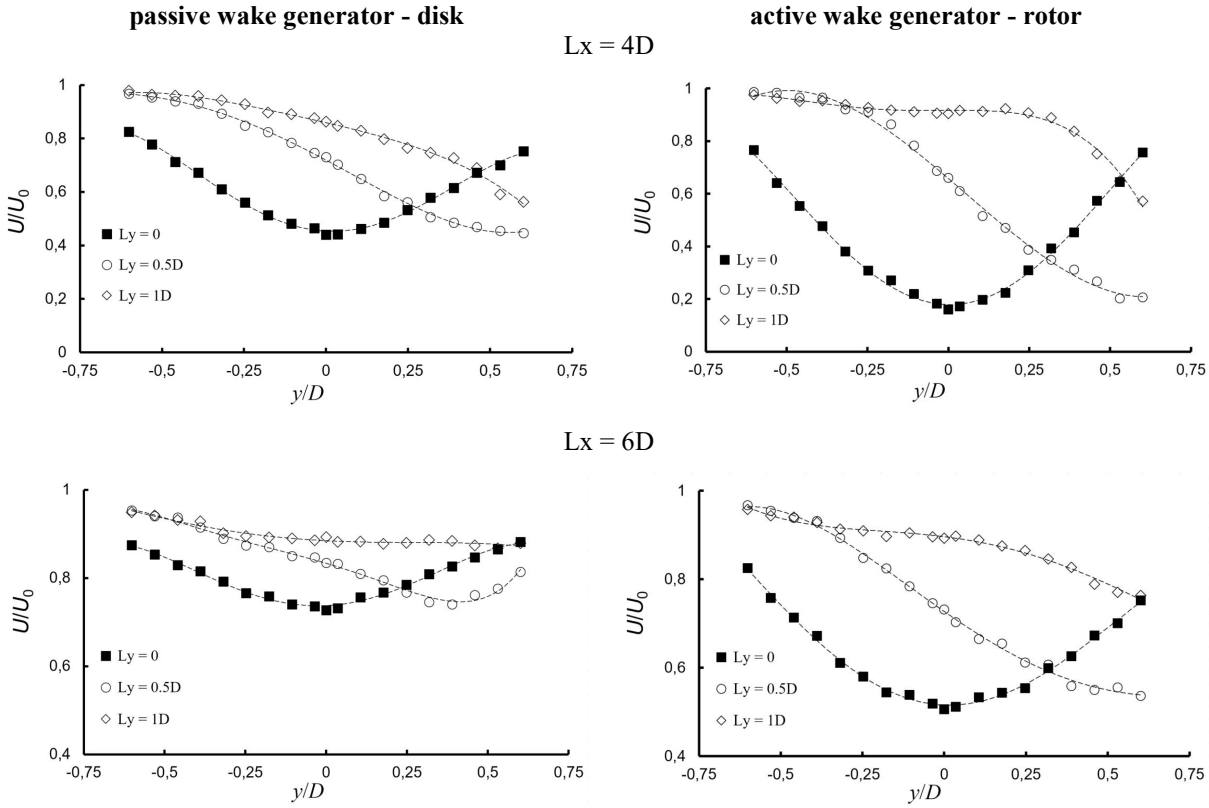

Figure 4. Wake velocity profiles at the different axis shifts behind passive (left) or active wake generators (right).

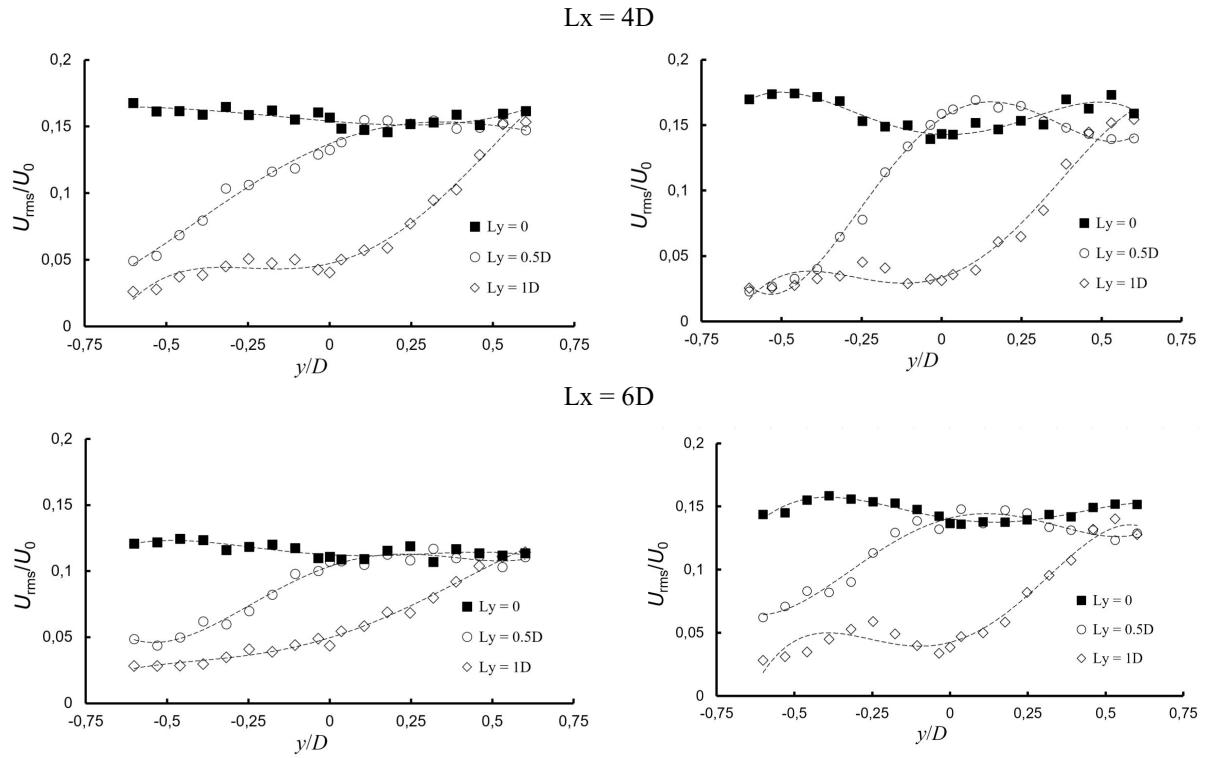

Figure 5. RMS in the wakes at the different axis shifts behind passive (left) or active wake generators (right).

3. Developments of the flow and rotor pulsations

The largest flow fluctuations (about 15 %) upstream of the tested rotor are observed at the minimum axial distance between the wake generators and tested rotor (Lx = 4D) when both rotors are coaxial (fig. 5). By increasing Lx to 6D and Ly=0, the pulsations decreases 3 % in the passive disk wake and only to 1% behind the active rotor wake. With increasing Ly, the wake pulsations also decreases to 5 % for Ly=0.5 and for Ly =1D they become less 4-5 % for both types of the wake generators and both values of Lx (fig. 5).

An influence of both wakes on the power and thrust of the tested rotor was examined too (fig. 6,7). Measurements of the rotor characteristics, torque (M) and thrust (T), were collected by strain sensors installed in the rotor mounting [9, 10]. The voltage of the sensors was amplified by a preamplifier Scout 55, produced by Hootinger Baldwin Messtechnik, and was digitized by the ADC produced by National Instruments Company. Both strain sensors were calibrated with an inaccuracy of less than one percent using reference weights. This system recorded the electrical signal of the strain sensors with a frequency of 120 Hz for 60 s. The obtained data served to calculate average values of the torque (M) and thrust (T) acting on the rotor axis. An evolution of the optimal operating regimes for the second tested rotor placed into both wakes generated by the passive immobile disk or the active rotating rotor were achieved (fig. 6).

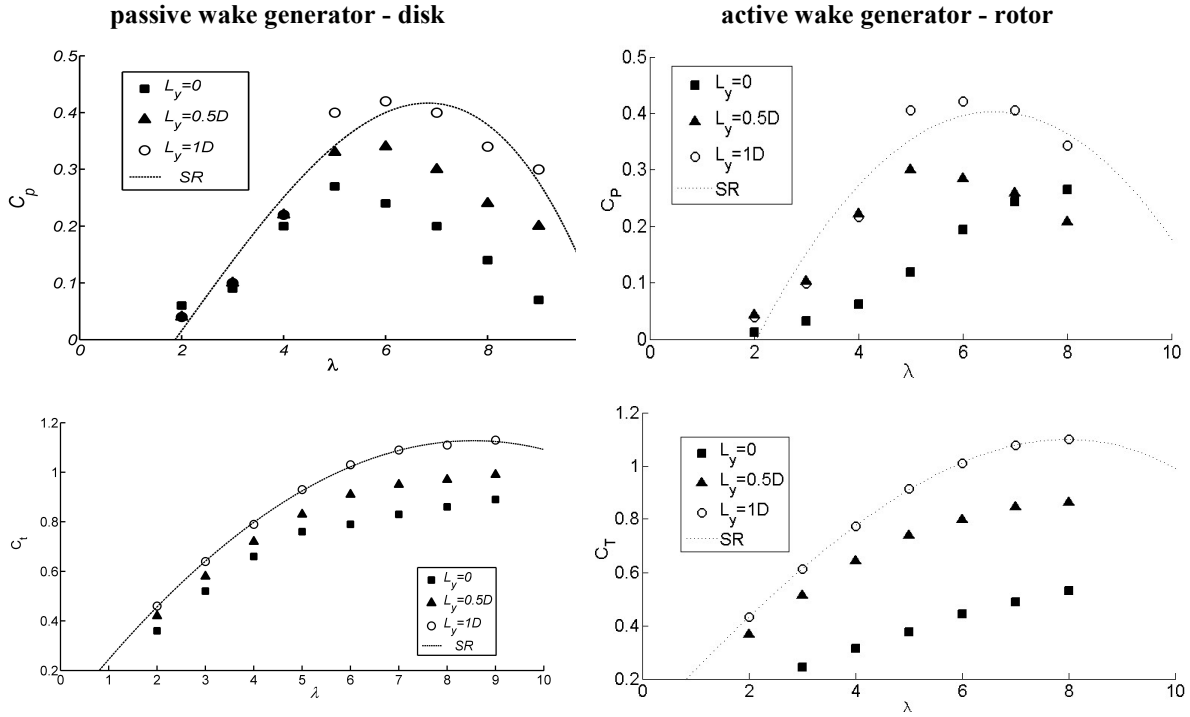

Figure 6. Power C_P and trust C_T coefficients of the tested rotor at Lx=6D and in different wakes.

For the single rotor, an angular velocity of the servo drive n_0 = 2.29 rps, coincides to the design TSR of the single rotor (λ_0 = 5) with the maximal power coefficient C_{P0}= 0.37 and the incoming free stream flow (U_0 = 0.54 m/s). The dependencies of Fig. 6 show that the wakes behind both the disk and rotor strongly influence on the rotor performance when the rotor axis coincides with the wake axis (Ly = 0) or contains in the wake (Ly = 0.5D). An impact of these wakes decreases also with an increasing of Lx (table 1). At Ly = 0.5D the rotor is situated in the half of the wake and C_P is rising. At Ly = 1D the rotor does not feel the influence of the wake and take values as the single rotor.

Table 1. Operating parameters of the dual setups.

Types of the setup	Parameters	Values						
	L_x - *distance*	4*D*			6*D*			8*D*
	Ly - distance	0	0.5*D*	1*D*	0	0.5*D*	1*D*	0
D-R (at $\lambda_2 = 5$)	*max* C_P/ C_{P0}	0.48	0.8	1	0.69	0.85	1	0.83
	Ct/ Ct_0	0.65	0.87	1	0.83	0.9	1	0.95
	Ct_2, RMS,%	18.6	9.77	3.14	15.9	9.39	4.44	6.94
R-R (at $\lambda_2 = 5$)	*max* C_{P2}/ C_{P0}	0.11	0.7	0.99	0.39	0.75	1	0.51
	Ct_2/ Ct_0	0.66	0.73	0.99	0.62	0.81	1	0.74
	Ct_2, RMS,%	18.54	10.08	3.08	14.29	9.54	3.57	7.95

The data's on figure 6 and table 1 shows that both the passive disk wake and the active rotor wake almost don't influence on the rotor performance when Ly = 1D. The power and trust coefficients in this case is almost equal to the single rotor value (solid curve).

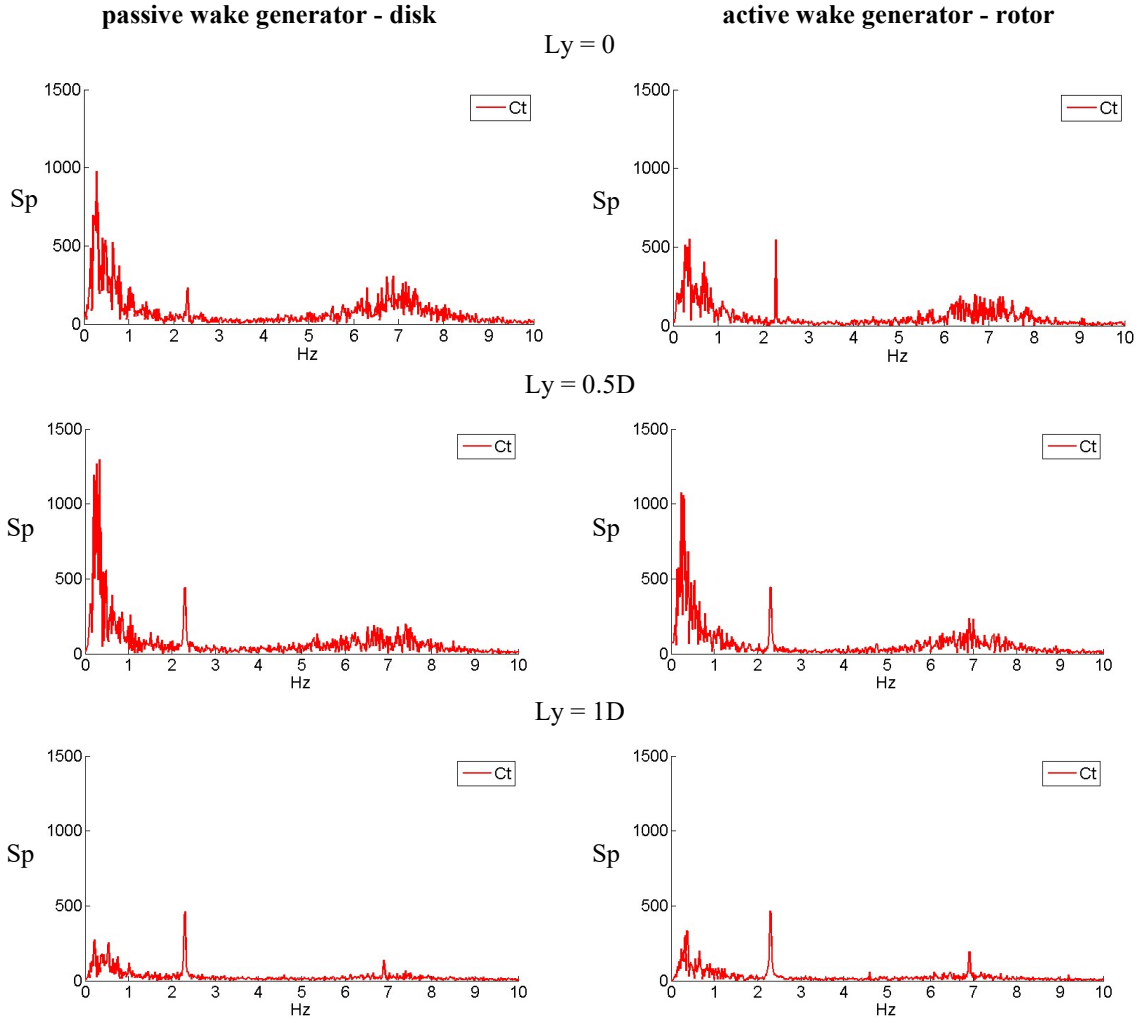

Figure 7. The spectra of C_T signal of rotor at λ_2=5 for of Lx=4 and different Ly, located in passive wake (left) or active wake (right).

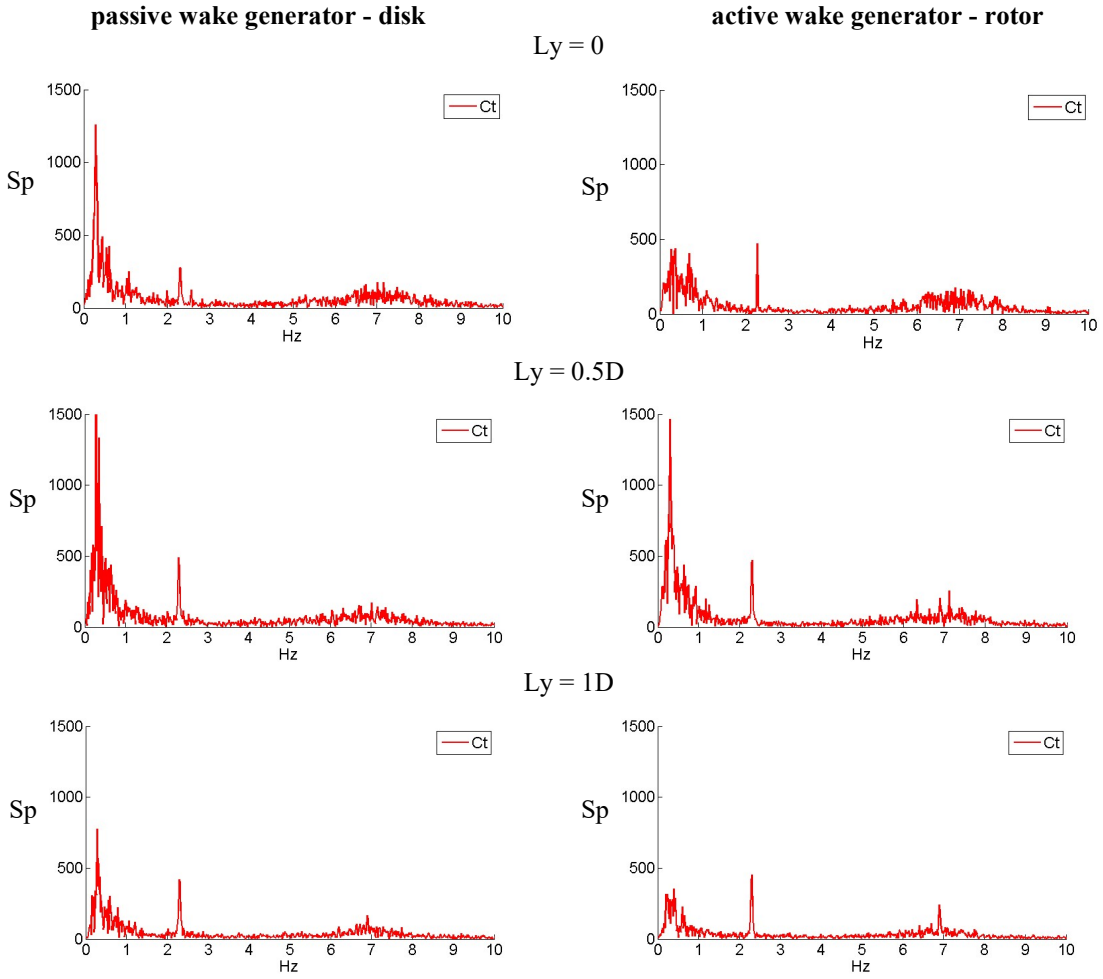

Figure 8. The spectra of C_T signal of the rotor at λ_2=5 Lx=6 and different Ly, located in the passive wake (left) or active wake (right).

The existence of strong oscillations (fig. 7, 8) was found on the same frequency of 0.27 Hz for all spectra of the C_T of the tested rotor, a value that correspond well to the Strouhal oscillation in both disk or rotor wakes [10]. Furthermore, computing spectra of the C_T of the tested rotor, a signal with frequencies of the rotation (2.29 Hz) and blade-rotation (6.87 Hz) itself was found too. For the Lx = 4D and Ly = 0 case, the spectra of C_T rotor frequency peak is greater than for the obstacle -disk case. This situation is caused by the upstream rotor wake influence, because the upstream rotational rotor speed was the same as for rotor one. However, for other cases of Lx and the none optimal regime of the first rotor operation, the spectra have not indicated any frequencies coming from the upstream rotor with the interactions of the active wake behind the first rotor.

The Strouhal frequency usually takes a dominant role in the spectra of the tested rotor placed inside of the passive wakes (Ly = 0 or 0.5D) and the value is about three times higher than the rotating or blade frequencies. In the active wake, the same behavior of the Strouhal frequency inherits only the case Ly = 0.5D. In the active wakes with the coaxial position of the tested rotor at Lx =4D and 6D, the Strouhal frequency does not take the dominant value in the spectra. An explanation of the different behavior of both spectra in the coaxial positions can be also connected with the different wake development in the case of the dual coaxial configuration from disks and rotors founded in [12].

At Ly =1D, when the tested rotor is not situated into the both wakes, the Strouhal frequency also become unimportant and both spectra becomes similar which coincides with the conclusion of an

insignificant impact on the average values of the torque (M) and thrust (T) of the outside rotor position from the wakes (fig. 6 and table 1).

4. Conclusions

An interaction between the axial-flow turbine and wakes generated by the disk and rotor placed upstream of the tested rotor was experimentally studied to estimate an influence of both passive and active obstacles on the rotor vibrations. The LDA measurements of the incoming flow have shown that the velocity attenuation by the passive wake generator – immobile disk is less than for the active wake generator – spinning rotor. The rms measured by LDA before the tested rotor has shown that the flow pulsations behave in the same manner for both types of the obstacle. The power of the tested rotor placed in the disk wake is greater than one in the rotor wake. The spectra of the rotor vibrations have shown an existence of the Strouhal frequency, the rotor and blade frequencies of the rotation itself, but they have not indicated any frequencies inherited the upstream rotor.

The obtained results are of interest for further development of aerodynamics of the wind farm where the turbine interactions with the wakes behind other turbines.

5. Acknowledgments

The research was supported by the Russian Science Foundation (Project № 14-19-00487).

References

[1] Thomas A. Wind Power in Power systems. *John Wiley and sons, ltd.* 2005:1120.
[2] Port-Agel F,Wu YT, Chen CH. A numerical study of the effects of wind direction on turbine wakes and power losses in a large wind farm. *Energies*. 2013; 6(10): 5297–5313.
[3] Chamorro LP, Hill C, Neary VS, Gunawan B, Arndt REA, Sotiropoulos F. Effects of energetic coherent motions on the power and wake of an axial-flow turbine. *Physics of Fluids* 2015; 27(5): 055104.
[4] Troldborg N, Larsen GC, Madsen, HA, Hansen KS, Sørensen JN, Mikkelsen R. Numerical simulations of wake interaction between two wind turbines at various inflow conditions. *Wind Energy* 2011; 14: 859-876.
[5] Bartl J, Pierella F, Sætran L. Wake measurements behind an array of two model wind turbines. *Energy Procedia* 2012; 24:305-312.
[6] Breton SP, Nilsson K, Olivares-Espinosa H, Masson C, Dufresne L, Ivanell S. Study of the influence of imposed turbulence on the asymptotic wake deficit in a very long line of wind turbines. *Renewable Energy* 2014; 70: 153-163.
[7] Okulov VL, Naumov IV, Mikkelsen RF, Sørensen JN. Wake effect on a uniform flow behind wind-turbine model. *J. of Physics: Conference series.* 2015; 625: 012011.
[8] Naumov IV, Kabardin IK, Mikkelsen RF, Okulov VL, Sørensen JN. Rotor performance and wake conditions in non-uniform flow behind an obstacle. *Journal of Physics: Conference Series* 2016; 753: 032051
[9] Naumov IV, Mikkelsen RF, Okulov VL. Estimation of Wake Propagation behind the Rotors of Wind-Powered Generators. *Thermal Engineering* 2016; 63(3): 208–213.
[10] Okulov VL, Naumov IV, Mikkelsen RF, Kabardin IK, Sørensen JN. A regular Strouhal number for large-scale instability in the far wake of a rotor. *J. Fluid Mech.* 2014; 747: 369-380.
[11] Naumov IV, Litvinov IV, Mikkelsen RF, Okulov VL. Investigation of a wake decay behind a circular disk in a hydro channel at high Reynolds numbers. *Thermophysics and Aeromechanics* 2015; 22(6): 657-665.
[12] Okulov VL, Mikkelsen RF, Naumov IV, Litvinov IV, Gesheva E, Sørensen JN. Comparison of the far wake behind dual rotor and dual disk configurations. Journal of Physics: Conference Series 2016; 753: 032060.